DIFFRACTION TOMOGRAPHY USING ARBITRARY TRANSMITTER AND RECEIVER SURFACES[1]

A. J. Devaney and G. Beylkin

Schlumberger-Doll Research
P. O. Box 307
Ridgefield, CT 06877

The theory of diffraction tomography for two-dimensional objects within the Born approximation is presented for cases where the scattered field is measured over arbitrarily shaped boundaries surrounding the object. Reconstruction algorithms are presented for both plane wave (parallel beam) and cylindrical wave (fan beam) insonification. Special attention is devoted to cases where the measurement and source boundaries are either lines or circles. The theory and algorithms presented are shown to be readily extended to the case of three-dimensional objects.

Key words: Diffraction tomography; filtered backpropagation; fan beam tomography

1. INTRODUCTION

The theory of diffraction tomography within the Born and Rytov approximations is usually

2 and 3. In figure 2 the object is still insonified by plane waves but the scattered field measurements are performed over arbitrarily shaped surfaces surrounding the object- one surface for each direction of plane wave insonification. In figure 3 the object is surrounded by an arbitrarily shaped surface Σ_0 on which are placed point sources. The scattered field measurements are then performed over arbitrarily shaped surfaces surrounding the object- one surface for each location of the point source. In the case of figure 2 the object's properties are to be reconstructed from the totality of scattered field measurements performed in a sequence of experiments employing a full or partial set of insonifying plane waves. In the case of figure 3 the reconstruction is to be performed from the scattered field data generated as the point source covers a whole or part of the surface Σ_0. In either case the measurement surface Σ can remain fixed throughout the sequence of experiments or, alternatively, can vary from experiment to experiment.

presented in Section 2. For the sake of simplicity only two-dimensional objects will be considered here and throughout the remainder of the paper. The final section describes how the results

Fourier transform of the "object profile" evaluated on circles in Fourier space which are the two-

proportional to the spatial Fourier transform of the scattered field over the measurement line. Finally, an inversion formula is presented that allows the object profile to be reconstructed from the scattering amplitude specified over a range of insonifying wave directions. For the classical tomographic configuration the scattering amplitude can be expressed in terms of the scattered field

13th International Acoustical Imaging Symposium, October 26-28, 1983.

0161-7346/84 $3.00

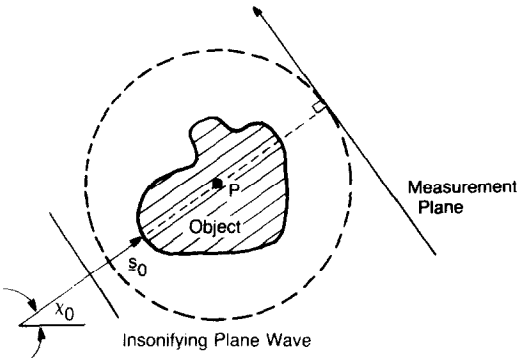

Fig. 1 Classical tomographic configuration. Measurement plane rotates about a central point "P" remaining always parallel with the insonifying plane wavefront.

2. DIFFRACTION TOMOGRAPHY WITHIN THE BORN APPROXIMATION

We consider the situation illustrated in figure 2 of an acoustic object surrounded by an arbitrary measurement surface Σ. We shall limit our attention to those applications where the wave propagation is governed by the inhomogeneous Helmholtz equation

$$(\nabla^2 + k^2)\psi(\underline{r}) = k^2 O(\underline{r})\psi(\underline{r}) \ . \tag{1}$$

Here, $k = \omega/C_0$ is the wavenumber of the field in the medium surrounding the object at frequency ω and $O(\underline{r})$ is the "object profile." For acoustic scattering, Eq. (1) applies if the density of the object is constant and equal to that of the embedding medium and if the shear modulus of the

however, be generalized to the non constant density case following the treatment presented in [8].

the z axis) but vary in perpendicular directions (say over the x-y plane). We will also assume that

x-y plane. Cylindrical waves having axes aligned parallel to the z axis are considered in Section 4. For both of these cases the field $\psi(\underline{r})$ will depend only on the x-y coordinates so that the wave equation (1) is a two-dimensional equation.

The object profile $O(\underline{r})$ is the quantity which is to be determined in diffraction tomography. This quantity is related to the velocity profile $C(\underline{r})$ of the object through the equation [4]

$$O(\underline{r}) = 1 - \frac{C_0^2}{C^2(\underline{r})} \ , \tag{2}$$

where C_0 is the velocity of the embedding medium. In general the velocity $C(\underline{r})$ will be a real

The goal of diffraction tomography is to reconstruct $O(\underline{r})$ from scattered field measurements. The most compact and convenient form of such data is given by the so-called plane wave scattering amplitude of the object. For the case of two dimensional objects, the plane wave scattering amplitude is defined via the equation

$$f(\underline{s}, \underline{s}_0) \equiv k^2 \int d^2r \ O(\underline{r})\psi(\underline{r}; \underline{s}_0)e^{-ik\underline{s}\cdot\underline{r}} \ , \tag{3}$$

where $\underline{s}_0$ and $\underline{s}$ are two-dimensional unit vectors that can range over the entire unit circle. In the above definition $\psi(\underline{r}; \underline{s}_0)$ is the total field (incident plus scattered) generated by an insonifying plane wave whose unit propagation vector is $\underline{s}_0$. Throughout this and the following section we shall refer to $f(\underline{s},\underline{s}_0)$ as simply the "scattering amplitude."

for those values of $\underline{s}$ lying on the half unit circle $s_x \geq 0$. More specifically, one finds that for

$$f(\underline{s}, \underline{s}_0) = 2i\gamma \ e^{-i\gamma|_0} \int_{-\infty}^{\infty} d\xi' \ \psi^{(s)}(\xi'; \underline{s}_0)e^{-i\kappa\xi'} \ , \tag{4}$$

where ξ' denotes position along the measurement line and $\psi^{(s)}(\xi' \cdot s_\perp)$ is the scattered field at the

the direction of $\underline{s}_o$; i.e.,

$$\text{generalized } \hat{\xi} \tag{5a}$$

$$\gamma = k\underline{s} \cdot \underline{s}_o = \sqrt{k^2 - \kappa^2}\,, \tag{5b}$$

where $\hat{\xi}$ denotes the unit vector in the positive ξ direction. (Recall that for the classical [illegible] has generalized (4) to the case of arbitrarily shaped measurement boundaries. As shown by Porter, the generalization to such cases requires, in general, that **both** the scattered field and its normal derivative **be measured** over the surface. We shall present, in the following section, a generalization of Eq. (4) to arbitrarily shaped measurement boundaries that differs somewhat from the extension proposed by Porter [10].

[illegible] tomography. Within the Born approximation, $f(\underline{s}, \underline{s}_o)$ reduces to the two-fold spatial Fourier transform of $O(\underline{r})$ evaluated over certain circular boundaries in Fourier space (Ewald spheres in the [illegible] $\exp(ik\underline{s}_o \cdot \underline{r})$ for $\psi(\underline{r}, \underline{s}_o)$ in Eq. (3) (i.e., making the Born approximation). We obtain [4]

$$f(\underline{s}, \underline{s}_o) \approx k^2 \int d^2r\, O(\underline{r}) e^{-ik(\underline{s}-\underline{s}_o)\cdot\underline{r}} = k^2 \tilde{O}[k(\underline{s}-\underline{s}_o)] \tag{6}$$

where

$$\tilde{O}(\underline{K}) \equiv \int d^2r\, O(\underline{r}) e^{-i\underline{K}\cdot\underline{r}} \tag{7}$$

denotes the two-fold spatial Fourier transform of the object profile.

Eq. (6) states that the scattering amplitude $f(\underline{s}, \underline{s}_o)$ determines the two-fold Fourier transform of the object profile over the locus of $\underline{K}$ values defined by the equation

$$\underline{K} = k(\underline{s} - \underline{s}_o)\,. \tag{8}$$

For fixed k and $\underline{s}_o$, Eq. (8) defines a locus of $\underline{K}$ values lying on a circle centered at $\underline{K} = -k\underline{s}_o$ and having a radius equal to k. As discussed in references 4 and 5, the above result is, essentially, the generalization of the projection-slice theorem of x-ray tomography to diffraction tomography and forms the basis for all reconstruction algorithms presently employed in diffraction tomography. For example, for the conventional tomographic configuration $f(\underline{s}, \underline{s}_o)$ is determined for unit vectors $\underline{s}$ [illegible]

from the scattering amplitude without the need of interpolation or Fourier inversion. In the case of two-dimensional objects the formula is given by [4, 5, 14]

$$O_{LP}(\underline{r}) = \frac{1}{2(2\pi)^2} \int_{-\pi}^{\pi} d\chi_o \int_{-\pi}^{\pi} d\chi \sqrt{1-(\underline{s}\cdot\underline{s}_o)^2}\, f(\underline{s}, \underline{s}_o) e^{ik(\underline{s}-\underline{s}_o)\cdot\underline{r}}\,, \tag{9}$$

where χ_o and χ are, respectively, the angles formed by $\underline{s}_o$ and $\underline{s}$ with a fixed reference direction. The subscript "LP" on $O(\underline{r})$ means that a "low pass filtered" approximation to the object profile is obtained; i.e.,

$$O_{LP}(\underline{r}) = \frac{1}{(2\pi)^2} \int_{K<2k} d^2K\, \tilde{O}(\underline{K}) e^{i\underline{K}\cdot\underline{r}}\,. \tag{10}$$

$$\hat{O}(\underline{r};\chi_o) \equiv \frac{1}{4\pi}\int_{-\pi}^{\pi} d\chi\sqrt{1-(\underline{s}\cdot\underline{s}_o)^2}\, f(\underline{s},\underline{s}_o)e^{ik(\underline{s}-\underline{s}_o)\cdot\underline{r}}. \tag{11a}$$

It then follows from Eq. (9) that $O_{LP}(\underline{r})$ is given by

$$O_{LP}(\underline{r}) = \frac{1}{2\pi}\int_{-\pi}^{\pi} d\chi_o \hat{O}(\underline{r};\chi_o). \tag{11b}$$

The construction of $\hat{O}(\underline{r};\chi_o)$ according to Eq. (11a) can be interpreted as a filtered backpropagation process while Eq. (11b) represents a sum over view angles [4, 5].

3. PARALLEL BEAM INSONIFICATION

from field measurements performed over the arbitrary measurement boundary Σ. The function $f(\underline{s},\underline{s}_o)$ so obtained can then be employed in Eq. (9) (or, equivalently in Eqs. (11)) to obtain a reconstruction of the object profile.

Porter [10] has addressed this problem and proposed a scheme which is a two-step procedure

entirely these two steps. We make use of the following integral identity which is derived in Appendix A.

$$k^2\int d^2r' O(\underline{r}')\psi(\underline{r}')e^{-ik\underline{s}\cdot\underline{r}'}$$

$$= \int_\Sigma dl'[ik\hat{\underline{n}}'\cdot\underline{s}\,\psi^{(s)}(\underline{r}') + \frac{\partial}{\partial n'}\psi^{(s)}(\underline{r}')]e^{-ik\underline{s}\cdot\underline{r}'}. \tag{12}$$

on Σ, $\hat{\underline{n}}'$ the unit outward normal vector to Σ at the point $\underline{r}'$ and $\frac{\partial}{\partial n'}$ denotes the derivative along the $\hat{\underline{n}}'$ direction. The field $\psi(\underline{r}')$ is the total field (incident plus scattered) generated by any incident wave to the object $O(\underline{r})$ and $\psi^{(s)}$ is the scattered wave component of ψ; i.e., the total field minus the incident field.

Since $\psi(\underline{r}')$ is the total field generated by any incident wave to the object we are free to choose the incident wave to be the plane wave $\exp(ik\underline{s}_o\cdot\underline{r}')$. For this choice $\psi(\underline{r}') = \psi(\underline{r}',\underline{s}_o)$ and the left-

$$f(\underline{s},\underline{s}_o) = \int_\Sigma dl'[ik\hat{\underline{n}}'\cdot\underline{s}\,\psi^{(s)}(\underline{r}';\underline{s}_o) + \frac{\partial}{\partial n'}\psi^{(s)}(\underline{r}',\underline{s}_o)]e^{-ik\underline{s}\cdot\underline{r}'}. \tag{13}$$

Eq. (13) allows the scattering amplitude to be evaluated directly in terms of the scattered field and

measure **both** $\psi^{(s)}$ and $\frac{\partial}{\partial n'}\psi^{(s)}$ on Σ. Moreover, in theory it is not necessary since it can be shown that either one alone uniquely determines the other [15].

In practice it is possible to obtain an exact relationship between the scattering amplitude $f(\underline{s},\underline{s}_0)$ [illegible] $\frac{\partial}{\partial n'}\psi^{(s)}$ [illegible]

of such boundaries, called "separable boundaries", are circles and infinite straight lines. For [illegible] Eq. (13) [illegible] Eq. (4). This [illegible]

Eq. (13) exactly cancels the integral involving $\frac{\partial}{\partial n'}\psi^{(s)}$ if $\hat{\underline{n}}'\cdot\underline{s} < 0$, and the two are equal if $\hat{\underline{n}}'\cdot\underline{s} \geq 0$ [16]. Thus, we have the general result that for all $\underline{s}$ such that $\hat{\underline{n}}'\cdot\underline{s} \geq 0$

$$f(\underline{s},\underline{s}_0) = 2ik\,\hat{\underline{n}}'\cdot\underline{s}\int_{-\infty}^{\infty} dl'\,\psi^{(s)}(l';\underline{s}_0)e^{-ik\underline{s}\cdot\underline{r}}\,, \tag{14}$$

where we have denoted by $\psi^{(s)}(l';\underline{s}_0)$ the scattered field $\psi^{(s)}(\underline{r}';\underline{s}_0)$ evaluated on the measurement line. Eq. (4) is then a special case of (14) for the classical tomographic configuration where $\hat{\underline{n}}' = \underline{s}_0$, the direction of propagation of the insonifying plane wave.

For the case of a circular boundary one finds that Eq. (13) reduces to [16]

$$f(\underline{s},\underline{s}_0) = 4i\int_0^{2\pi} d\sigma\,\psi^{(s)}(\sigma;\underline{s}_0)F_R(\chi-\sigma)\,. \tag{15}$$

where R is the radius of the measurement circle Σ assumed to be centered at the origin and σ and [illegible] denotes the scattered field at the angle σ and the function $F_R(x)$ is given by

$$F_R(x) = \frac{1}{(2\pi)^2}\sum_{n=-\infty}^{\infty}\frac{i^n}{H_n(kR)}e^{inx} \tag{16}$$

where H_n is the n'th order Hankel function of the first kind. It should be noted that the center and radius of Σ can be changed as a function of the insonifying wave vector $\underline{s}_0$.

An approximate expression for $f(\underline{s},\underline{s}_0)$ for arbitrarily shaped boundaries which involves only the scattered field can be employed if the boundary curvature is such that it can be approximated by a straight line in the vicinity of each point. This requires that the local radius of curvature be much larger than a wavelength. If this condition is met then the arguments leading to Eq. (14) for the case when Σ is a straight line can be applied and Eq. (13) then reduces, approximately, to

$$f(\underline{s},\underline{s}_0) \approx 2ik\int_{\Sigma} dl'\,\hat{\underline{n}}'\cdot\underline{s}\,\psi^{(s)}(\underline{r};\underline{s}_0)e^{-ik\underline{s}\cdot\underline{r}}\,, \tag{17}$$

where $\hat{\underline{n}}'\cdot\underline{s}$ must now remain under the integral sign since $\hat{\underline{n}}'$ is not constant for a curved boundary.

4. CYLINDRICAL BEAM INSONIFICATION

In this section we consider the case where the object is insonified by a cylindrical wave generated by a line source located on a closed boundary Σ_0 surrounding the object. For parallel beam insonification the object profile is reconstructed from scattered field measurements performed over an arbitrary boundary Σ surrounding the object. A reconstruction of the object profile is obtained from the set of scattered field measurements that result from using different directions of insonification of the incident wave (different unit wave vectors $\underline{s}_0$). For the cylindrical beam case we will also assume that the scattered field is measured over an arbitrary boundary which completely surrounds the object. The object profile reconstruction is then obtained from the set of scattered field measurements that result when the location of the line source varies over Σ_0.

We shall present two alternative schemes for generating a reconstruction of the object profile

second method combines the two steps into a single mathematical operation. What results is then a filtered backpropagation algorithm where the "sum over view angles" operation is replaced by a "sum over source points" operation. This second method is the diffraction tomographic equivalent of the fan beam filtered backprojection algorithm of x-ray tomography [17].

We begin by defining, in analogy with Eq. (3), the cylindrical wave scattering amplitude $\gamma(\underline{s};\underline{R}_o)$ of the object:

$$\gamma(\underline{s};\underline{R}_o) \equiv k^2 \int d^2r\, O(\underline{r})\, \psi(\underline{r};\underline{R}_o) e^{-ik\underline{s}\cdot\underline{r}}. \tag{18}$$

plays the same role with respect to insonifying cylindrical waves as does the plane wave scattering amplitude $f(\underline{s},\underline{s}_o)$ for insonifying plane waves.

$$\gamma(\underline{s};\underline{R}_o) = \int_\Sigma dl' \left[ik\hat{\underline{n}}'\cdot\underline{s}\,\psi^{(s)}(\underline{r}';\underline{R}_o) + \frac{\partial}{\partial n'}\psi^{(s)}(\underline{r}';\underline{R}_o)\right] e^{-ik\underline{s}\cdot\underline{r}'}, \tag{19}$$

which is the cylindrical wave counterpart to Eq. (13). Because Eq. (19) is mathematically identical to Eq. (13), the arguments leading to Eqs. (14), (15) and (17) remain valid for Eq. (19). In particular, we have for straight line measurement boundaries the result

and for circular boundaries

and, finally, for boundaries with weak curvature:

$$\gamma(\underline{s},\underline{R}_o) \approx 2ik \int_\Sigma dl'\, \hat{\underline{n}}'\cdot\underline{s}\, \psi^{(s)}(\underline{r}';\underline{R}_o) e^{-ik\underline{s}\cdot\underline{r}'}. \tag{20c}$$

The cylindrical wave scattering amplitude $\gamma(\underline{s},\underline{R}_o)$ is seen to be linearly related to the scattered wave $\psi^{(s)}(\underline{r}';\underline{R}_o)$ generated by an insonifying cylindrical wave. Moreover, the scattered field $\psi^{(s)}(\underline{r}';\underline{s}_o)$ produced by an insonifying plane wave can be shown to be linearly related to the scattered field $\psi^{(s)}(\underline{r}';\underline{R}_o)$ produced by line sources located on Σ. As a consequence of this, the

$$f(\underline{s},\underline{s}_o) = \int dl \left[ik\,\hat{\underline{n}}\cdot\underline{s}\,\gamma(\underline{s};\underline{R}_o) - \frac{\partial}{\partial n}\gamma(\underline{s};\underline{R}_o)\right] e^{ik\underline{s}_o\cdot\underline{R}_o} \tag{21}$$

where dl_o is the differential length on Σ_0, $\hat{n}_o$ the unit outward normal to Σ_0 and $\frac{\partial}{\partial n_o}$ denotes the derivative along the $\hat{n}_o$ direction.

Eq. (21) is in the form of a linear mapping between the cylindrical wave scattering amplitude and its derivative with respect to n_o and the plane wave scattering amplitude $f(s, s_o)$. Since the

important to remove this quantity from Eq. (21). This can be done exactly for cases where Σ_0 is a

$$f(s, s_o) = -\frac{k}{2} \hat{n}_o \cdot s_o \int_{\Sigma_0}^{\infty} dl_o \, \gamma(s; l_o) e^{iks_o \cdot R_o} \qquad (22)$$

with Eq. (22) holding for all s_o such that $\hat{n}_o \cdot s_o \leq 0$ and where l_o now denotes the location of R_o on the straight line boundary. The relationship between Eqs. (22) and (21) is seen to be entirely analogous to that existing between Eqs. (14) and (13) of Section 2. Indeed, Eq. (22) is derived

becomes [16]

$$f(s, s_o) = \int d\beta \, \gamma(s; \beta) F_{R_o}(\beta - \chi_o) \, , \qquad (23)$$

where $F_{R_o}(\gamma)$ is defined in Eq. (16) with R replaced by R_o and where β and χ_o are respectively the angles formed by R_o and s_o with an arbitrary reference direction. Finally, for cases where the curvature of the boundary Σ_0 is sufficiently small that it can be approximated by a straight line in the vicinity of each point; we have

$$f(s, s_o) \approx -\frac{k}{2} \int_{\Sigma_0} dl_o \, \hat{n}_o \cdot s_o \, \gamma(s; R_o) e^{iks_o \cdot R_o} \, . \qquad (24)$$

Eqs. (19)-(24) allow the plane wave scattering amplitude to be synthesized from cylindrical wave scattering data. The cylindrical wave scattering amplitude is first computed using (19) or (20) and

Σ_0 are straight lines or circles and for cases where the curvature of both boundaries is small.

The transformations listed in table I allow the plane wave scattering amplitude to be synthesized from cylindrical wave scattered field data. Once $f(s, s_o)$ is computed the plane wave filtered backpropagation algorithm as embodied in Eqs. (9) or (11) can be employed to obtain a reconstruction of the object profile. An alternative, one step reconstruction algorithm, is readily derived by substituting the transformations listed in table I into Eq. (9) and reorganizing the result. We present in table II the resulting reconstruction algorithms corresponding to the three cases - lines, circles and weakly curving boundaries - covered in table I.

The reconstruction algorithms presented in table II are "fan beam" algorithms in the sense that they operate directly on the measured cylindrical wave scattered field data. Like the plane wave filtered backpropagation algorithm presented in Section 2, they can be decomposed into two sequential operations:

1. Generating a partial reconstruction using data collected in a single scattering experiment.
2. Summing the partial reconstructions obtained in step 1 from different experiments to obtain the final reconstruction.

Eqs. (19)-(24) allow the plane wave scattering amplitude to be synthesized from cylindrical wave scattering data. The cylindrical wave scattering amplitude is first computed using (19) — (20) and

Table I. Scattering amplitudes in different

Σ_o, Σ lines	$= -ik^2(\hat{n}_o\cdot\underline{s}_o)(\hat{n}'\cdot\underline{s})\int_{-\infty}^{\infty}dl_o\int_{-\infty}^{\infty}dl'\psi^{(s)}(l';l_o)e^{-ik(\underline{s}\cdot\underline{r}'-\underline{s}_o\cdot\underline{R}_o)}$
Σ_o, Σ circles	$= 4i\int_{-\pi}^{\pi}d\beta\int_{-\pi}^{\pi}d\sigma\,\psi^{(s)}(\sigma;\beta)F_R(\chi-\sigma)F_{R_o}(\beta-\chi_o)$
Σ_o, Σ arbitrary but with weak curvature	$= -ik^2\int_{-\infty}^{\infty}dl_o(\hat{n}_o\cdot\underline{s}_o)\int_{-\infty}^{\infty}dl'(\hat{n}'\cdot\underline{s})\psi^{(s)}(\underline{r}';\underline{R}_o)e^{-ik(\underline{s}\cdot\underline{r}'-\underline{s}_o\cdot\underline{R}_o)}$

the result is employed in Eqs. (22)-(24) to compute $f(\underline{s},\underline{s}_o)$. By combining these equations, the two steps can be combined into a single integral transform relating the cylindrical wave scattering data directly to the plane wave scattering amplitude. Table I lists these transforms for cases where Σ and

from cylindrical wave scattered field data. Once $f(\underline{s},\underline{s}_o)$ is computed the plane wave filtered backpropagation algorithm as embodied in Eqs. (9) or (11) can be employed to obtain a reconstruction of the object profile. An alternative, one step reconstruction algorithm, is readily derived by substituting the transformations listed in table I into Eq. (9) and reorganizing the result

Table II. Reconstruction formulae in different cases of source-receiver geometry

Geometry	Reconstruction
Σ_o, Σ lines	$O_{LP}(\underline{r}) = \int_{-\infty}^{\infty}dl_o\int_{-\infty}^{\infty}dl'\psi^{(s)}(l';l_o)G_p(\underline{r};l',l_o)$, where $G_p(\underline{r};l',l_o)\equiv -\frac{ik^4}{2(2\pi)^2}\int_{-\pi}^{\pi}d\chi_o\int_{-\pi}^{\pi}d\chi(\hat{n}_o\cdot\underline{s}_o)(\hat{n}'\cdot\underline{s})\sqrt{1-(\underline{s},\underline{s}_o)^2}e^{ik\underline{s}\cdot(\underline{r}-\underline{r}')}e^{-ik\underline{s}_o\cdot(\underline{r}-R_o)}$
Σ_o, Σ circles	$O_{LP}(\underline{r}) = \int_{-\pi}^{\pi}d\beta\int_{-\infty}^{\infty}d\sigma\,\psi^{(s)}(\sigma;\beta)G_c(\underline{r};\sigma,\beta)$, where $G_c(\underline{r};\sigma,\beta)\equiv\frac{2ik^2}{(2\pi)^2}\int_{-\pi}^{\pi}d\chi_o\int_{-\pi}^{\pi}d\chi\sqrt{1-(\underline{s}\cdot\underline{s}_o)^2}\,F_{R(\chi-\sigma)}F_R(\beta-\chi_o)e^{ik(\underline{s}-\underline{s}_o)\cdot\underline{r}}$
Σ_o,Σ arbitrary but with weak	$O_{LP}(\underline{r}) \approx \int_{-\infty}^{\infty}dl_o\int_{-\infty}^{\infty}dl'\,\psi^{(s)}(\underline{r}';\underline{R}_o)G_p(\underline{r};\underline{r}',\underline{R}_o)$, where

The reconstruction algorithms presented in table II are "fan beam" algorithms in the sense that they operate directly on the measured cylindrical wave scattered field data. Like the plane wave filtered backpropagation algorithm presented in Section 2, they can be decomposed into two sequential operations:

1. Generating a partial reconstruction using data collected in a single scattering experiment.
2. Summing the partial reconstructions obtained in step 1 from different experiments to obtain the final reconstruction.

In table II the inner integral represents step 1 while the sum over partial reconstructions is performed by the outer integral. In the plane wave case, the sum over experiments consisted of summing over different insonifying angles χ_o. Clearly, for fan beam insonification (cylindrical wave insonification) the sum over experiments corresponds to an integral over source points $\underline{R}_o$.

We conclude by remarking that the fan beam reconstruction algorithm for circular boundaries given in table II is the generalization, to diffraction tomography, of the x-ray fan beam algorithm presented, for example, in [17]. The parallel beam filtered backpropagation algorithm of diffraction tomography is known to reduce, in the limit where the wavelength goes to zero, to the filtered backprojection algorithm of x-ray tomography [4]. It should then be expected that the circular boundary fan beam algorithm in table II should, likewise, reduce in this limit to the corresponding X-ray algorithm. We have not yet been able to establish this reduction and consider this an interesting and important future research goal for fan beam diffraction tomography.

5. CONCLUDING REMARKS

reconstruction procedures for fan beam diffraction tomography. The first of these is a two-step inversion algorithm where plane wave scattering data is synthesized from cylindrical wave scattering data in the first step and the object profile is reconstructed in the second step using the parallel beam (plane wave) filtered backpropagation algorithm on the synthesized plane wave data. The second algorithm combines these two steps into a single "fan beam filtered backpropagation

locations.

The results presented in the paper apply only to two-dimensional objects; i.e., objects whose

dimensional case. This extension can be performed in two ways. The first of these simply requires

boundary Σ is a circular cylinder while for a line boundary Σ becomes a plane surface. The treatment presented in the paper then applies for three-dimensional objects enclosed by $\hat{\Sigma}$ if the two-dimensional scattered field measurements performed over $\hat{\Sigma}$ are **projected** onto the boundary Σ. The resulting reconstruction will be of a projection of the three-dimensional object profile onto

plane as the boundary Σ. This first method is the generalization, to the case of arbitrary measurement boundaries, of the three-dimensional reconstruction method presented in Section 4 of

The theory and algorithms presented here can also be generalized to the three-dimensional case

defined by

$$f(\underline{s},\underline{s}_0) = k^2 \int d^3r\, O(\underline{r})\psi(\underline{r};\underline{s}_0)e^{-ik\underline{s}\cdot\underline{r}}, \tag{25}$$

where now $\underline{r} = (x,y,z)$ and $s = (s_x,s_y,s_z)$. Eqs. (4)-(8) are similarly generalized to the three-

dimensional case. The three-dimensional form of the inversion formula (9) is given by [14,18].

[redacted]

$$(2\pi)$$

where $d\Omega_{s_0}$ and $d\Omega_s$ are differential solid angles and the integrals are over 4π steradians. By employing Eq. (26) together with the appropriate three-dimensional generalization of the expressions for the scattering amplitude given in table I, three-dimensional reconstruction algorithms analogous to those given in Table II can be readily obtained.

APPENDIX A - DERIVATION OF EQ. (12)

We begin by setting $\psi(\underline{r})$ in Eq. (1) equal to the sum of an insonifying wave $\psi^{(i)}(\underline{r})$ and a scattered wave $\psi^{(s)}(\underline{r})$. Since the insonifying wave satisfies the homogeneous Helmoltz equation; i.e., Eq. (1) with $O(\underline{r}) = 0$, we find that

$$(\nabla^2 + k^2)\psi^{(s)}(\underline{r}) = k^2 O(\underline{r})\psi(\underline{r}) \ . \tag{A.1}$$

We can obtain a relationship between the scattered field $\psi^{(s)}$ and its normal derivative $\frac{\partial}{\partial n}\psi^{(s)}$ evaluated on the boundary Σ by making use of Eq. (A.1) and the fact that $\exp(-ik\underline{s}\cdot\underline{r})$ satisfies the homogeneous Helmholtz equation, i.e.,

$$(\nabla^2 + k^2)e^{-ik\underline{s}\cdot\underline{r}} = 0 \ . \tag{A.2}$$

[redacted]

$$= k^2 O(\underline{r})\psi(\underline{r})e^{-ik\underline{s}\cdot\underline{r}} \ . \tag{A.3}$$

Integrating with respect to $\underline{r}$ throughout the volume of space bounded by Σ and applying Green's theorem then yields

$$k^2 \int d^2r \ O(\underline{r})\psi(\underline{r})e^{-ik\underline{s}\cdot\underline{r}} = \int_\Sigma dl \left\{ e^{-ik\underline{s}\cdot\underline{r}} \frac{\partial}{\partial n}\psi^{(s)}(\underline{r}) - \psi^{(s)}(\underline{r}) \frac{\partial}{\partial n} e^{-ik\underline{s}\cdot\underline{r}} \right\} . \tag{A.4}$$

In this equation $\frac{\partial}{\partial n}$ denotes differentiation along the outward normal to the boundary Σ and dl is

$$\frac{\partial}{\partial n} e^{-ik\underline{s}\cdot\underline{r}} = -ik\,\hat{\underline{n}}\cdot\underline{s}\, e^{-ik\underline{s}\cdot\underline{r}} \ , \tag{A.5}$$

we finally obtain

$$k^2 \int d^2r \, O(\underline{r})\psi(\underline{r})e^{-ik\underline{s}\cdot\underline{r}}$$

$$= \int_\Sigma dl \left[\frac{\partial}{\partial n}\psi^{(s)}(\underline{r}) + ik\hat{\underline{n}}\cdot\underline{s}\,\psi^{(s)}(\underline{r}) \right] e^{-ik\underline{s}\cdot\underline{r}} \tag{A.6}$$

which is the desired result.

APPENDIX B - DERIVATION OF EQ. (21)

The wavefield $\psi(\underline{r}';\underline{r})$ generated by a line source centered at $\underline{r}'$ satisfies the equation

[redacted]

where $\nabla_{\underline{r}}^2$ denotes the Laplacian operator in the $\underline{r}'$ coordinates. The field $\psi(\underline{r}';\underline{s}_0)$ generated by the

[redacted]

Upon multiplying Eq.(B.1) by $\psi(\underline{r}';\underline{s}_0)$ and Eq. (B.2) by $\psi(\underline{r};\underline{r}')$ and subtracting the two resulting equations yields

$$\psi(\underline{r}';\underline{s}_0)\nabla_{\underline{r}}^2\psi(\underline{r};\underline{r}') - \psi(\underline{r};\underline{r}')\nabla_{\underline{r}}^2\psi(\underline{r}';\underline{s}_0)$$

$$= \psi(\underline{r}';\underline{s}_0)\,\delta(\underline{r}-\underline{r}') \ . \tag{B.3}$$

[6] Lipson, H. and Cochran, W., *The Determination of Crystal Structures* (Cornell University

[9] Woll, E., Three-dimensional structure determination of semi-transparent objects from holographic data, Opt. Commun. 1, 153-156 (1969).

[10] Porter, R., Determination of structure of weak scatterers from holographic images, Opt. Commun. 39, 362-364 (1981).

[11] Mueller, R. K., Kaveh, M., and Inverson, R. D., A New Approach to Acoustic Tomography

(Plenum Press, New York, 1980).

[12] Pan, S. X. and Kak, A. C., A computational study of reconstruction algorithms for diffraction tomography, *IEEE Trans. Acoustics, Speech and Signal Processing* (to appear).

[13] Slaney, Malcolm and Kak, A. C., Diffraction tomography, in *Inverse Optics*, A. J. Devaney, ed., *Proc. SPIE Vol. 413*, pp. 2-19 (1983).

[14] Beylkin, G., The fundamental identity for iterated spherical means and the inversion formula

T75

York, 1953).

[16] Beylkin, G. and Devaney, A. J., Theory of diffraction tomography within the Born and Rytov approximations, submitted to J. Math. Phys.

[17] Kak, A. C., Computerized tomography with x-ray emission and ultrasound sources, *Proc. IEEE 67*, 1245-1272 (1979).

[18] Devaney, A. J., Inversion formula for inverse scattering within the Born approximation, *Opt. Lett. 7*, 111-112 (1982).